Pramana – J. Phys. (2016) 87: 89
DOI 10.1007/s12043-016-1291-x

Complex plasma experimental device – A test bed for studying dust vortices and other collective phenomena

MANJIT KAUR[1,2,*], SAYAK BOSE[1], P K CHATTOPADHYAY[1], J GHOSH[1] and Y C SAXENA[1]

[1]Institute for Plasma Research, Bhat, Gandhinagar 382 428, India
[2]Present address: Department of Physics and Astronomy, Swarthmore College, 500 College Ave., Swarthmore, PA 19081, USA
*Corresponding author. E-mail: angel.manjit@gmail.com

MS received 8 July 2015; revised 29 January 2016; accepted 7 March 2016; published online 3 November 2016

Abstract. A typical device for carrying out sophisticated and complex dusty plasma experiments is designed, fabricated and made operational at the Institute for Plasma Research, India. The device is named as complex plasma experimental device (CPED). The main aim of this multipurpose machine is to study the formation and behaviour of dust vortices in the absence of external magnetic field under the effect of various plasma parameters. Further, the device is equipped with advanced imaging diagnostics for studying many other interesting phenomena such as dust oscillations, three-dimensional crystalline structures, dust rotation, etc. The device is quite flexible to accommodate many innovative experiments. Detailed design of the device, its diagnostics capabilities and the advanced image analysis techniques are presented in this paper.

Keywords. Dusty plasma; vortices; particle image velocimetry technique; glow discharge.

PACS No. 52.27.Lw

1. Introduction

Continuous matter in nature is often observed to form spontaneous self-organized structures. These self-organized structures can be easily observed in complex (dusty) plasmas where micron-sized dust particles get levitated in plasma after getting charged and arrange themselves in an organized fashion. These organized structures influence many observable critical or collective phenomena, like formation of Coulomb crystals [1,2], transition of dust medium from crystalline to liquid phase [3] or formation of voids and self-organized structures [4] and dust rotation or vortices. The dust vortices occurring in complex (dusty) plasma experiments are ideal test beds for studying turbulence in fluids with low Reynolds number. The studies related to the formation of dust vortex are very important and would lead to proper understanding of many physical phenomena such as fluid flow through a regular porous medium [5] and the flow of elastic polymer solutions [6]. Also in dusty plasmas, the dynamics of the dust vortices with different shapes can be analysed on the very kinetic level, which is of practical importance as well of interest for studying the basic physics of vortices when these are created by flows around an obstacle. The dust vortices can be produced in laboratory as well as in microgravity experiments. In microgravity experiments [4], dust vortices are observed generally around a dust-free region. However, it is difficult to perform these experiments routinely because of the limited operational time and high costs involved. Also, lot of preparation is needed for a single campaign. In laboratory experiments (under the effect of gravity), these can be generated by immersing a biased probe [7] in plasma or by using laser beams [8]. These can also be produced by generating a temperature gradient in the background neutral gas due to free convection [9] at high pressure or due to thermal creep flow [10,11] at low pressures. In these experiments, the surrounding plasma parameters can be determined using electric probes as they still serve as the primary work-horse for local measurements of electron temperature and plasma density in low-temperature plasmas.

At Institute for Plasma Research, an experimental set-up, named as complex plasma experimental device

(CPED), has been developed in which the dust vortices can be generated in the absence of any external magnetic field and studied in detail using electrical as well as optical diagnostics. The important feature of this set-up is that in this device, the dust vortices are produced in the absence of external magnetic field, or biased probe or any temperature gradient in the surrounding gas. Thus, this set-up can act as an ideal low-cost test-bed for studying the phenomena of generation of dust vortices typically similar to those generated under microgravity experiments. This set-up is equipped with a specially designed Langmuir probe system, capable of working in a dusty plasma environment at high pressures, and a sophisticated high-resolution camera with high frame grabbing capability, in order to perform direct measurements of the surrounding plasma parameters and the properties of the dust particles. Although dust vortices have been observed in several experiments, the principal mechanism behind their formation, their evolution and dependency on the background plasma parameters as well as on neutral concentration is still not fully understood. In order to address these issues, special care has been taken in designing the subsystems of the experimental set-up.

The whole paper has been arranged as follows: In §2, we describe the basic considerations for the construction of this device along with the detailed design of the subsystems such as electrical diagnostics, imaging camera, dust particles used, etc. In §3, the techniques used for analysing the experimental data obtained using the specialized sCMOS camera are provided. Section 4 discusses about the electrical characteristics of the plasma and provides some interesting experimental results obtained at different pressures. Conclusion is provided in §5.

2. Experimental set-up

2.1 *Vacuum vessel and electrode system*

The experiments are being carried out in a stainless steel cylinder of 31 cm diameter and 50 cm length as shown in figure 1. The cylinder is equipped with four radial ports which are used for various purposes such as for evacuating the vacuum vessel, for feeding working gas, for inserting the electrode system and carrying out their electrical connections, for passing the laser sheet to illuminate the dust particles and for inserting electrical diagnostics for the determination of the background plasma properties. The vacuum vessel consists of two large diameter axial ports with glass windows mounted on them. Through one of the axial glass ports, sCMOS camera images the dynamics of the micron-sized dust particles moving or rotating at high speeds. The other axial port is used for imaging by a DSLR camera or for carrying out spectroscopic measurements.

The device is capable of accommodating three different types of plasma sources, namely RF discharge, cold cathode glow discharge and hot filament discharge. Depending upon the physics issue to be studied, any one of these plasma sources can be used. Radiofrequency as well as filament-produced plasmas are also well suited for studies related to crystalline structures and wave studies at low pressures as the

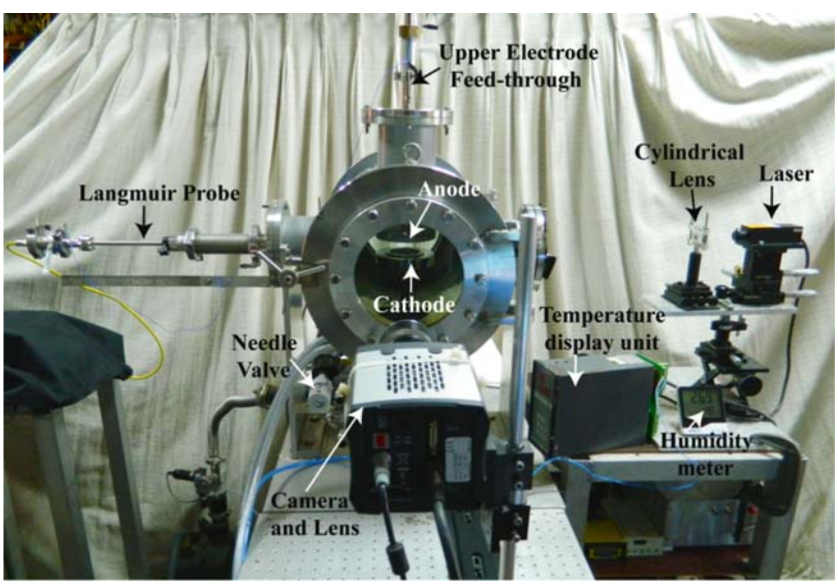

Figure 1. Photograph of the experimental set-up with different subparts.

plasma remains quieter in terms of inherent fluctuations. The RF-produced plasmas are diagnosed using RF-compensated probes.

In the present paper, we shall describe only the parallel plate DC glow discharge plasma operation that has been used for creating and studying dust vortices. The discharge is being produced between two horizontal parallel plate electrodes made of stainless steel. The upper electrode, inserted in the vacuum vessel from the top radial port along with its electrical connections, is a disc of 10 cm outer diameter and acts as the live anode. Its edges are covered by a boron nitride cup. Thus, only the front part of the anode is used for the plasma production with an exposed diameter of 9 cm. The lower electrode, introduced through the bottom radial port into the vacuum vessel, is a disc of 13 cm diameter and acts as a grounded cathode. The whole body of the cylindrical system along with the lower electrode acts as a grounded cathode. Due to ion bombardment on the surface of the cathode, its temperature rises which can further alter the surrounding plasma properties in various ways. This heating of cathode surface gives rise to a temperature gradient in the surrounding gas neutrals and can affect the dynamics of dust particles. Actively water-cooled electrode has been used to get rid of this temperature gradient in the neutral gas. Also by using active water cooling, the cathode surface can be maintained at different temperatures, resulting in different temperature gradients in the neutral gas which further provides the facility for studying its effect on the plasma parameters as well as on the dust dynamics in a very controlled manner. For creating a flexibility of controlling the temperature gradient created by ion bombardment externally, the lower electrode has been designed in a very special way to have the provision of active water cooling. For determining its surface temperature, a thermocouple has been installed on it. The dimensions of the electrodes and the interelectrode separation are chosen in such a way that plasma production occurs mainly between the electrodes rather than between the anode and the vessel walls. The interelectrode separation that can be varied from 1 to 10 cm, is kept fixed as 4 cm for the results presented in this paper. For creating a radial density inhomogeneity in the plasma, a metallic ring with an inner diameter as 63 mm, an outer diameter as 82 mm and the height above cathode surface as 3 mm is kept on the lower electrode. The lower electrode has a groove on its surface to keep the metallic ring concentric. The metallic ring is in good electrical as well as thermal contact with the lower electrode as it sits tightly in the groove on the lower electrode.

The vacuum system is evacuated using a rotary pump that maintains a base pressure less than 1 Pa. For feeding argon gas to the vacuum system and for varying neutral density in it, a needle valve that is mounted on one of the KF25 ports present on the bottom radial port, is used. Provision of injecting the working gas in the vacuum system from the bottom port and evacuating it through the same port is done to avoid any directed flow of neutral gas in the experimental region of interest as doing so allows only diffused gas to enter the system. After evacuating the vacuum vessel, the working gas (i.e., argon gas) is purged into it a number of times at high pressures to reduce the background gas impurities. During the experiments, the pressure of argon gas is varied between 20 Pa and 350 Pa using the needle valve. The discharge voltage is varied from 270 V to 420 V to keep the discharge current in the range of 1 mA to 40 mA. To avoid vibrations of the rotary pump (from disturbing the vacuum system), a non-vibrating bellow is used to connect it to the vacuum vessel. In these experiments, no external magnetic field is applied.

2.2 *Selection of dust particles*

In dusty plasmas, the dust particles can be levitated at certain heights by maintaining a balance between the gravitational pull due to the weight of the dust particles and the force due to sheath electric field in the opposite direction. Dust particles having diameter $\leq 1\ \mu$m can easily be levitated in weak sheath electric fields (~ 0.06 V cm^{-1} for the individual dust particle of charge $q_{\mathrm{d}} \sim 8 \times 10^3 e^-$). However, it is very difficult to illuminate as well as locate these small dust particles using imaging techniques. Bigger particles of diameter $> 10\ \mu$m can easily be illuminated and located properly using imaging techniques, but stronger sheath electric fields are required to make them levitate (~ 6.2 V cm^{-1} for individual dust particle of charge $q_{\mathrm{d}} \sim 8 \times 10^4 e^-$ as $q_{\mathrm{d}} \propto r_{\mathrm{d}}$ and $m_{\mathrm{d}} \propto r_{\mathrm{d}}^3$). Based on the magnitudes of the sheath electric fields in DC glow discharge near the cathode sheath, dust particles with diameters in the range of 3–9 μm are found to be best suitable for conducting experiments.

Generally, dielectric dust particles are used in experiments rather than metallic particles as they can be distributed over the metallic electrodes whereas the metallic dust particles only have to be sprinkled from top using dust-shaker. Furthermore, the metallic dust particles, heavier than the dielectric particles of the same size due to their higher mass densities, thus require higher electric fields to get levitated.

Based on these considerations and depending upon the availability of standard sizes, monodispersive melamine formaldehyde (MF) particles of 6.48 μm diameter are used in the present experiments due to their excellent monodispersivity (CV $<$ 3%) and highly uniform spherical shapes. Approximately 1 g of monodispersed MF dust particles are spread uniformly on the cathode surface up to the inner diameter of the metallic ring using a mesh as the levitation of dust particles is found to be sensitive to the distribution of dust particles on the cathode. These particles have a low mass density ($\sim$1.51 g cm^{-3}), are resistant up to high temperatures ($\sim$300°C) and do not agglomerate easily. Apart from MF particles, silica particles of approximately same size as that of the MF particles are also used in some of the experiments. Silica particles also have a low mass density ($\sim$1.8–2 g cm^{-3}) and are resistant to high temperatures ($\sim$1000°C).

2.3 *Camera and laser*

For imaging the dust particles using a high-speed camera, the dust particles should be illuminated using a light source. A 100 mW @ 532 nm laser is used to illuminate the dust particles. To illuminate a broader section of the levitated dust particles, the laser beam is converted into a vertical laser sheet of around 1–2 mm thickness using a cylindrical lens. The laser sheet illuminates the levitated dust torus which is formed in the experiments and described later, along its diameter and enables us to see its two diametrically opposite poloidal planes which basically look like two vertical dust rings/clouds. The light coming from the dust rings/clouds is captured by sCMOS Neo® camera.

In order to study the physics underlying the formation of dust vortices, three-dimensional structures, waves and oscillations, it is not sufficient to produce them, but sophisticated diagnostics and analysis tools are also required to extract accurate information from the experimental data. The choice of the camera depends on three very important parameters (other than the full well capacity, dynamic range, etc.). These three basic parameters are: (1) number of pixels on the camera chip, (2) size of each pixel and (3) frame rate of the camera. The field of view is decided by the number of pixels, pixel size and the lens used.

Focussing on the study of dust rotation, where locating each and every dust particle precisely for PIV analysis is of prime importance, the camera is chosen. In these experiments, the dust particles are expected to rotate in circular orbits at very high speed ($\sim$2–10 cm s^{-1}). To resolve the dust particles moving at such high speeds, the exposure time of the camera should be sufficiently small. Otherwise, the particles will travel over a number of pixels in a single exposure time and will appear as lines. At the same time, in order to capture complete dust structures, large field of view is necessary. In CPED, depending on the cathode and ring dimensions, field of view of $\sim 85 \times 40$ mm^2 is required for capturing the full dust-torus (i.e., both diametrically opposite poloidal planes). Apart from the rotation studies, locating the dust particles precisely and accurately to determine the interparticle separation between them is also important in studies related to various types of crystalline structures. The pair correlation function that tells about the various states of the dust structures (like fcc, hcp etc.) critically depends on the interparticle distances that need to be measured accurately. Therefore, to capture the rotating structures of the dust particles, a fast camera with a high frame grabbing rate (usually inverse of exposure time) and high resolution with pixel size comparable to the size of the particles and large number of pixels, is required.

Considering all the above prerequisites, a black & white Neo 5.5 sCMOS camera containing 2560×2160 pixels with each pixel as a square of size 6.5 μm is chosen for the experiments in CPED. The camera can deliver sustained 30 fps or up to 100 fps in burst mode at full resolution. The camera is equipped with 4 GB of on-head memory buffer. The memory buffer can store 400–500 frames corresponding to 4–5 s when the camera is operated at its full resolution and maximum frame grabbing rate capacity. For studying faster dust dynamics, the frame rate can be further increased by reducing the camera resolution (i.e., the effective number of pixels). For example, frame grabbing rate of $\sim$405 fps is achieved at a resolution of 512×512 pixels. For a fixed region of interest, higher kinetic series lengths are possible by lowering the frame grabbing rates. But, if both frame grabbing rate and kinetic series length are required to be increased simultaneously (for e.g., for determining the dust temperature), then the data must be spooled continuously to either the computer hard-drive or computer RAM with greater than 4 GB capacity.

The data from the camera are transferred to the computer hard-drive from the on-head buffer through a CameraLink cable of required transfer speed. The speed of data transfer is limited by the writing speed of the computer hard-drive. To increase the writing speed, the unused RAM of the computer is converted into a virtual hard-drive with much faster (∼50 times faster than the physical hard-drive) writing speeds using a special software RAMDisk. Later, the data are transferred to the conventional hard-drive.

For obtaining the required field of view (i.e., $\sim 85 \times 40$ mm^2), the camera is being used with a Carl Zeiss-made macrolens of 100 mm focal length. To increase the signal-to-noise ratio, a band-pass laser-line filter has been used between the camera and the macrolens, which attenuates the background plasma light and allows the laser light scattered from the dust particles to pass through it.

2.4 *Electric probes*

The background plasma plays an important role in the dynamics of dust particles embedded in it and hence should be characterized thoroughly for the proper understanding of dust rotation, crystalline structure formation etc. The background plasma of CPED is characterized using a specialized cylindrical Langmuir probes system. Movable single and double Langmuir probes are employed for determining plasma parameters such as plasma density, electron temperature and plasma potential. The double probe is a symmetric probe with two probe tips made up of tungsten wire of 1 mm diameter and 10 mm length. The two tips are separated by ∼10 mm, which is much greater than the plasma Debye length (∼200 μm for $n_i \cong 3 \times 10^9$ cm^{-3} and $T_e \cong 2$ eV). The single Langmuir probe is also made up of tungsten wire of 0.125 mm diameter and 5 mm length. The electron temperature is determined from the slope of the linear region of ln (I_e) vs. V_{Bias} and the density is determined from the ion saturation region using the 'modified TALBOT and CHOU theory' [12]. As the positive ion collection by a cylindrical Langmuir probe in medium and higher pressure plasmas is substantially affected by the ion collisions with the surrounding neutrals, care must be taken in the determination of plasma parameters. Ion collisions with neutrals affect the probe collection mainly in two ways: the ion–neutral collisions (1) decrease the ion current to the probe at higher pressures due to elastic scattering and (2) increase the ion current to the probe due to the destruction of their orbital motion at medium pressures. For the pressure range of operation in our experiments, the value of Knudsen number ($K_i = \ell_i/r_p$) varies from 0.5 to 0.2 and the value of Debye number ($D_\lambda = r_p/\lambda_{De}$) varies from 0.5 to 3, where ℓ_i is the ion–neutral mean free path, r_p is the radius of the probe and λ_{De} is the electron Debye length. This range of plasma operation falls within the range of validity of 'modified TALBOT and CHOU model' [12].

In dusty plasmas, the Langmuir probes suffer from contamination due to the deposition of dust particles on them. A probe biased positively with respect to the plasma potential attracts negatively charged dust particles towards it very efficiently. The dust particles stick to the probe surface and alter the current collecting area. This leads to misinterpretation of the *I*–*V* characteristics of the probe. To avoid contamination [13], Langmuir probe is maintained at a potential much less than the floating potential of the background plasma using a DC power supply. A triangular waveform is superposed on the DC bias at 200 Hz frequency to acquire the current–voltage (*I*–*V*) characteristics of the Langmuir probe. This is done to ensure that the time duration for which the probe bias is close to plasma potential is very small (<0.4 ms). Since the dust response time is very high (>40 ms), the dust particles will not be able to respond to this positive probe potential in such a small duration of time. As a result, probe contamination by dust particles is avoided.

3. Data analysis using PIV technique

To extract physics information such as dust rotation speed, direction of rotation, velocity distribution etc. from the images taken using the sCMOS camera, particle image velocimetry (PIV) technique is used. It is a cross-correlation technique for determining the displacement of particles between pair of images. In this technique, an image is first decomposed into 'interrogation cells' of $n \times n$ pixels, i.e., 8×8 pixels, 32×32 pixels, 128×128 pixels etc. such that a finite number of particles are present in each cell. Then a two-dimensional Fourier transform is performed on each cell on two consecutive images, say Image 1 and Image 2, and a cross-correlation is constructed between the two images. The peak of the cross-correlation represents the most probable displacement of the group of particles in the cell. It is noted that the cross-correlation calculation can result in multiple peaks. The 'quality' of the PIV analysis is measured as the ratio of the heights of the first and second cross-correlation peaks and for fluid systems, a ratio of 1.5 or greater is considered to be good. Ratios of 3 or greater have been used in the experiments reported here. The motion of a group of particles within the interrogation cell is represented by a vector. The cells are fixed in space whereas, the particles flow in and out of the cells.

4. Plasma characterization and preliminary results in CPED

After evacuation, the vacuum vessel is filled with the working gas (namely, Ar, Kr and He) to produce plasma. In the present paper, the results corresponding to Ar plasma are shown. The radially resolved horizontal probe measurements are made from one edge of the electrode to the centre at different heights above the cathode. The electron temperature and plasma density are found to be 2.5 eV and 2×10^9 cm^{-3} respectively. We have carried out a detailed electrical characterization of the discharge to identify the stable discharge conditions. In order to do so, Paschen curve is plotted (as shown in figure 2) which provides information about the dependence of breakdown voltage on the interelectrode separation and operating gas pressure.

The interelectrode separation is kept smaller than the transverse dimensions of the electrodes to minimize the fringing of the electric field between the two electrodes. In CPED, a detailed load-line analysis using different current limiting resistances has been done to identify the experimental conditions to keep the discharge in the normal regime of the glow discharge. In the normal regime of the glow discharge, the voltage drop across the electrode remains nearly constant with the variations in applied voltage and the discharge current vary proportionally to the variations in the applied voltage. In the case of low values of current limiting resistances, the discharge becomes very sensitive to any small change in the applied voltage which makes it difficult to work with. On the other hand, higher values of current limiting resistances put more demand on the power supply. For dusty plasma experiments, the current limiting resistance of $\sim$10 kΩ is used, with which an approximately constant voltage drop across the electrodes is achieved at a desired range of discharge current and pressure.

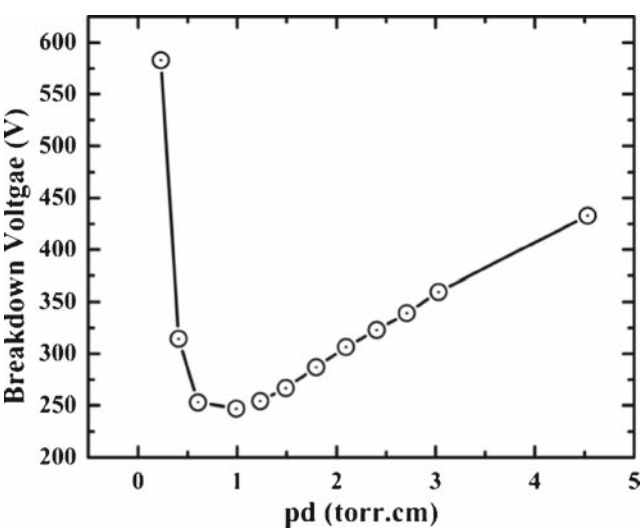

Figure 2. Paschen curve obtained in the present set-up at an interelectrode separation of 4 cm.

A number of experiments in CPED under different conditions have been carried out. In these experiments, no external perturbation to the system and no external magnetic field is applied. A number of different phenomena related to dust dynamics are observed by simply varying the working gas pressure and discharge current.

4.1 *Dust oscillations*

It is well known that in DC glow discharge experiments, spontaneous self-excited dust acoustic waves occur at pressures below certain pressure threshold (<40 Pa). These are a type of sound waves where inertia is provided by heavily charged dust particles and tension by ion and electron pressures. Above the threshold value, the increase in dust–neutral collisions severely damps these modes. At low pressures, where the neutral–dust collisions are considerably less, the ion drag force starts dominating and leads to larger amplitude dust-acoustic waves with concomitant non-linear effects. The experiments in CPED showed high-amplitude dust oscillations at comparatively low pressures ($\sim$20 Pa) as shown in figure 3. At these low pressures, the dust particle oscillations gain bigger amplitudes due to the dominance of ion drag and appear to be bouncing from the cathode surface resembling a dust-shower; the average velocity of the dust particles in these high-amplitude oscillations is $\sim$6 cm s^{-1}. It is to be noted here that the dust-acoustic waves and high-amplitude oscillations that occur in CPED are intrinsically generated without the application of any external perturbation.

4.2 *3D dust structures*

Stationary three-dimensional dust structures are easily produced in CPED at a pressure of $\sim$50 Pa. These

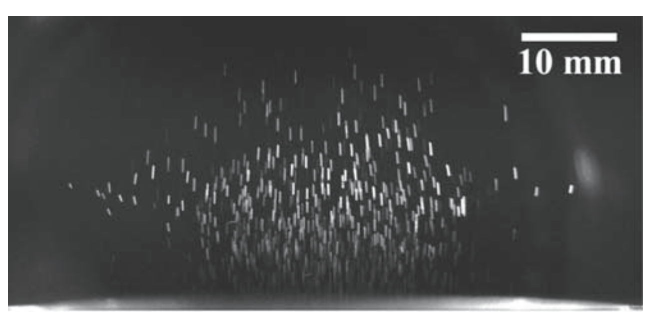

Figure 3. High-amplitude dust oscillations at very low pressures ($\sim$20 Pa).

structures are formed at the centre of the cathode along with the formation of dense dust clouds of very fine particles above the metallic ring. These structures are very stable and stay there as long as the discharge parameters remain constant. Although the structures are of conical shape, having three dimensions, as observed by horizontal laser scanning, figure 4 shows the vertical two-dimensional view of these structures illuminated by the two-dimensional vertical laser sheet. The height of the two-dimensional structure is ∼6 mm and width ∼4 mm. The nearest-neighbour distance in these structures appears to be the same vertically and is ∼0.7 mm. It has been observed that the 2D dust structures exhibit solid-like behaviour at higher pressures and at low discharge currents, and undergoes a phase transition to fluid state when the pressure or the discharge current is increased. The typical electron temperature and density of the background plasma in the vicinity of the dust structure at 37 Pa are 4.5 eV and $\sim 6 \times 10^8$ cm^{-3}. This transition from solid-like phase to fluid phase happens because of the increase in the dust particle temperature and can be studied with high precision in case of dusty plasmas due to large size and slow response time of the dust particles. The phenomenon of melting of dust structure with an increase in gas pressure is very unusual and can be understood in the following way.

The dielectric dust particles have been kept on the cathode surface. These particles cover the metallic central part of the cathode and do not let this area of cathode to participate in plasma production. At low pressures, the plasma diffuses towards the centre and cathode dark space (sheath) also forms at centre.

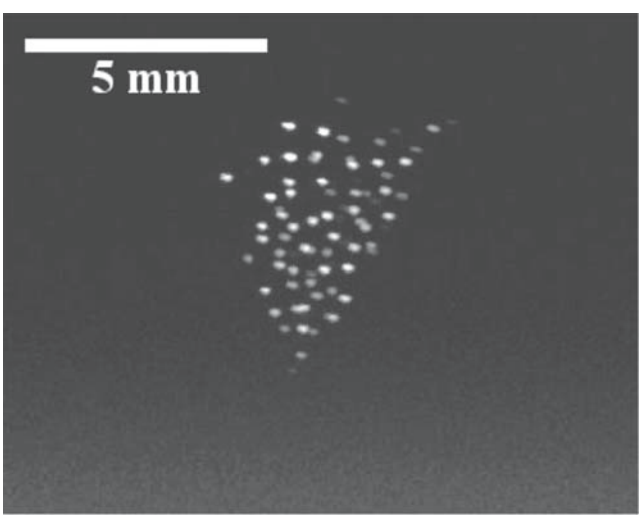

Figure 4. The image showing the vertical view of three-dimensional dust structures taken with the help of sCMOS camera.

With an increase in the pressure, the plasma diffusion towards the centre decreases, leading to a decrease in the plasma density. This further leads to a reduction in dust particle charge. The sheath field at the centre also weakens with an increase in the pressure. All these lead to a transition of the solid-like phase to a liquid-like phase leading to the disappearance of the three-dimesional structure.

4.3 *Dust-toroidal structures*

On increasing the pressure further up to 69 Pa, the thickness of the cathode sheath decreases further and a slanted horizontal sheet of dust particles forms above the sheath along with a stationary three-dimensional dust structure at the cathode centre. Beyond ∼70 Pa, the dust particles start showing mild rotation in the vertical plane and at 100 Pa, rotating dust clouds are formed. Two such fully grown rotating clouds at a pressure ∼110 Pa are visible near the diametrically opposite sides of the metallic ring as shown in figure 5 in *r*–*z* plane. Figure 5a has been recorded using sCMOS camera while figure 5b has been saved using DSLR camera. When the laser light is scanned in the horizontal plane, the images of the two rotating dust clouds get successively closer and merge into one cloud. The horizontal laser scanning along different chords over the cathode surface shows that the two dust clouds come close successively and merge to form a single cloud, indicating that the dust clouds are

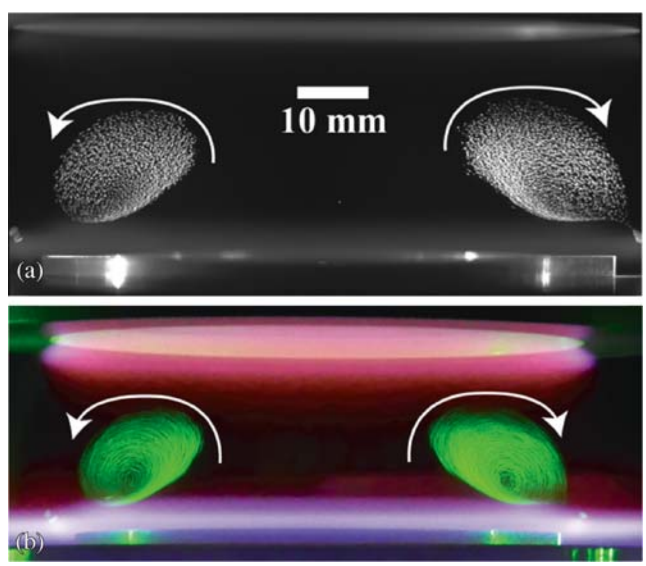

Figure 5. Two poloidal planes of the dust torus when illuminated using a vertical laser sheet along torus diameter taken (**a**) with help of a sCMOS camera and (**b**) with a visible DSLR camera.

toroidally continuous, which is confirmed by visual inspection. The particle image velocimetry (PIV) analysis of these images shown in figure 6 categorically indicates that the dust particle profile is similar to that of a rotating rigid body across the vortex line with shifted centre.

These structures are localized in the region where a sharp plasma density gradient exists [14]. The typical plasma parameters at 133 Pa are radial electric field (obtained from radial density gradient) $= \sim 1$ V cm^{-1}, electron temperature $= \sim 2$ eV and maximum density (near the outer edge of the metallic ring) $= \sim 4 \times 10^9$ cm^{-3} at a discharge current of 20 mA. The formation of dust-torus has been found to be extremely sensitive to the distribution of dust particles kept on the cathode inside the metallic ring. The direction of dust rotation in these structures depends upon the direction of the spatial density gradient. The dust cloud is confined in a region where a density gradient exists and the presence of density gradient is known to generate gradient in the ion drag force [14]. The gradient in the ion drag force produces a torque which makes the dust cloud to rotate. The direction of rotation is consistent with the direction of torque produced in the cloud. These dust rotations are observed without any external magnetic field and provides a very low-cost platform for studying the mechanism of generation of these rotations observed in microgravity experiments. In the same experiment, with a modification in the electrode geometry, we have managed to produce multiple dust vortices [15] confirming the role of density gradient in the formation of dust vortices.

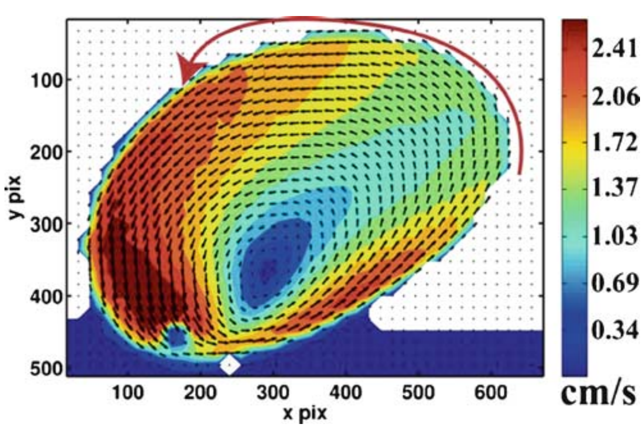

Figure 6. The velocity profile of the dust particles as an ensemble average of 479 flow fields obtained from PIV analysis with an interrogation window size of 32 × 32 at 50% overlap at 10.1 ms exposure time in one poloidal plane of the dust torus. The colour bar represents the magnitudes of dust velocities and the direction of arrows represents the direction of dust rotation.

5. Conclusion

A dedicated device for dusty plasma experiments is designed, fabricated and made operational at Institute for Plasma Research, India. Named as CPED, the aim of this multipurpose machine is to study the formation and behaviour of dust vortices in the absence of external magnetic field. Equipped with state-of-the-art imaging diagnostics, this device is quite flexible to accommodate many interesting and innovative phenomena related to dust oscillations, three-dimensional dust structures and phase transitions, intrinsic dust rotations, etc. Experiments on the formation of poloidally rotating toroidally symmetric dust vortices in the absence of external magnetic field in this device established the role played by gradients of ion drag force in dust cloud rotation along with the understanding of several other phenomena such as high-amplitude dust oscillations, dust acoustics modes, crystal structures etc.

References

[1] J H Chu and I Lin, *Phys. Rev. Lett.* **72**, 4009 (1994)
[2] H Thomas, G E Morfill, V Demmel, J Goree, B Feuer-bacher and D Mohlmann, *Phys. Rev. Lett.* **73**, 652 (1994)
[3] A Melzer, V A Schweigert, I V Schweigert, A Homann, S Peters and A Piel, *Phys. Rev. E* **54**, R46 (1996)
[4] G E Morfill, H M Thomas, U Konopka, H Rothermal, M Zuzic, A Ivlev and J Goree, *Phys. Rev. Lett.* **83**, 1598 (1999)
[5] N A Horton and D Pokrajac, *Phys. Fluids* **21**, 045104 (2009)
[6] A Groisman and V Steinberg, *Nature* **405**, 53 (2000)
[7] D A Law, W H Steel, B M Annaratone and J E Allen, *Phys. Rev. Lett.* **80**, 4189 (1998)
[8] M Klindworth, A Melzer, A Piel and V Schweigert, *Phys. Rev. B* **61**, 8404 (2000)
[9] M Schwabe, L-J Hou, S Zhdanov, A V Ivlev, H M Thomas and G E Morfill, *New J. Phys.* **13**, 083034 (2011)
[10] T M Flanagan and J Goree, *Phys. Rev. E* **80**, 046402 (2009)
[11] S Mitic, R Sutterlin, A V Ivlev, H Hofner, H M Thomas, S Zhdnov and G E Morfill, *Phys. Rev. Lett.* **101**, 235001 (2008)
[12] M Tichy, M Sicha, P David and T David, *Contrib. Plasma Phys.* **34**, 59 (1994)
[13] M Klindworth, O Arp and A Piel, *Rev. Sci. Instrum.* **78**, 033502 (2007)
[14] M Kaur, S Bose, P K Chattopadhyay, D Sharma, J Ghosh and Y C Saxena, *Phys. Plasmas* **22**, 033703 (2015)
[15] M Kaur, S Bose, P K Chattopadhyay, D Sharma, J Ghosh, Y C Saxena and E Thomas, *Phys. Plasmas* **22**, 093702 (2015)